Current Biology, Vol. 15, 79–85, January 11, 2005, ©2005 Elsevier Ltd. All rights reserved. DOI 10.1016/j.cub.2004.12.041

Ascidian *prickle* Regulates Both Mediolateral and Anterior-Posterior Cell Polarity of Notochord Cells

Di Jiang,[1] Edwin M. Munro,[2] and William C. Smith[1,*]
[1]Department of Molecular, Cellular, and Developmental Biology
University of California, Santa Barbara
Santa Barbara, California 93106
[2]Center for Cell Dynamics and
Friday Harbor Laboratories
University of Washington
620 University Road
Friday Harbor, Washington 98250

Summary

The ascidian notochord follows a morphogenetic program that includes convergent extension (C/E) followed by anterior-posterior (A/P) elongation [1–4]. As described here, developing notochord cells show polarity first in the mediolateral (M/L) axis during C/E, and subsequently in the A/P axis during elongation. Previous embryological studies [3] have shown that contact with neighboring tissues is essential for directing M/L polarity of ascidian notochord cells. During C/E, the planar cell polarity (PCP) gene products *prickle* (*pk*) and *dishevelled* (*dsh*) show M/L polarization. *pk* and *dsh* colocalize at the notochord cell membranes, with the exception of those in contact with neighboring muscle cells. In the mutant *aimless* (*aim*), which carries a deletion in *pk*, notochord morphogenesis is disrupted, and cell polarization is lost. After C/E, there is a dynamic relocalization of PCP proteins in the notochord cells with *dsh* localized to the lateral edges of the membrane, and *pk* and *strabismus* (*stbm*) at the anterior edges. An A/P polarity is present in the extending notochord cells and is evident by the position of the nuclei, which in normal embryos are invariably found at the posterior edge of each cell. In the *aim* mutant, all appearances of A/P polarity in the notochord are lost.

Results and Discussion

The notochord is one of the defining characteristics of the chordate phylum. During development of the ascidian larva, convergent extension (C/E) converts a four by ten sheet of developing notochord cells into a column of 40 stacked cells [2–4] (Figure 1A). Following C/E, notochord development continues as individual cells elongate in the anterior-posterior (A/P) axis, in part by secreting extracellular matrix into the spaces between neighboring cells [1]. Finally, these spaces fuse to form a tube that runs the length of the larval tail (Figures 1A and 1B). While much of notochord morphogenesis appears to be conserved among chordates, important differences exist between ascidians and vertebrates. The notochord cells in ascidians have completed the last round of cell division before C/E commences [2], while notochord cells in vertebrates continue to proliferate while C/E takes place [5]. Ascidian muscle cells, which border the notochord laterally, do not take part in C/E [2, 6], while vertebrate paraxial mesoderm undergoes C/E actively and contributes to the narrowing of embryo [5]. These differences, along with the relatively small number of cells involved, make ascidian embryos an attractive system in which to study the molecular mechanism underlying notochord morphogenesis. Here, we present the molecular cloning and analysis of the spontaneous recessive mutant *aimless* (*aim*) from the ascidian species *Ciona savignyi*. Embryos with the *aim* mutation carry a deletion in the *pk* gene. Embryos homozygous for *aim* fail to undergo normal C/E and post-C/E development.

Larvae homozygous for the *aim* mutation have dramatically shortened tails but no other obvious defects (Figure 1C). Confocal imaging of phalloidin-stained *aim/aim* embryos showed that the notochord fails to organize into a single-cell diameter column (Figures 1D and 1E). Organization of the notochord rudiment at late-gastrula stage, just prior to the commencement of C/E, appeared to be largely normal (Figures 1F and 1I). However, by neurula stage (7.25 hr postfertilization, [hpf]), when notochord cells normally start to converge and extend, *aim/aim* notochord cells began to show a marked difference from the wild-type (Figures 1G and 1J). Gene expression and histological examination of *aim/aim* embryos demonstrated that the differentiation of the muscle, endoderm, and nervous system proceeded normally (data not shown). Moreover, the notochords of *aim/aim* embryos expressed the differentiation gene *notochord-specific tropomyosin* [7] (data not shown), indicating that the *aim* phenotype is the result of a morphogenetic defect, rather than a tissue differentiation defect.

The swimming larval stage of *Ciona* persists for only a few days, at which point larvae attach by way of their anteriorly located adhesive palps and commence metamorphosis [1]. While *aim/aim* larvae had difficulty swimming, which severely hindered their ability to attach, those few that did attach were able to grow to fertile adults. Homozygotic *aim* adults produced 100% short-tailed offspring with no additional defects, indicating that the corresponding gene does not contribute maternally to development (data not shown).

A combination of positional cloning and candidate gene approaches were used to identify the mutant gene responsible for the *aim* phenotype. Amplified fragment length polymorphism (AFLP) fragments linked to the *aim* locus were identified by bulk segregant analysis (BSA) (Figure 2A), as described [8]. Three linked AFLP markers were found to cluster to a single 0.9 Mb scaffold of the partially assembled *C. savignyi* genome (http://www.broad.mit.edu/annotation/ciona/index.html) (Figure 2B). The gene encoding the *C. savignyi* homolog of the *Drosophila* planar cell polarity (PCP) gene *pk*, designated

*Correspondence: w_smith@lifesci.ucsb.edu

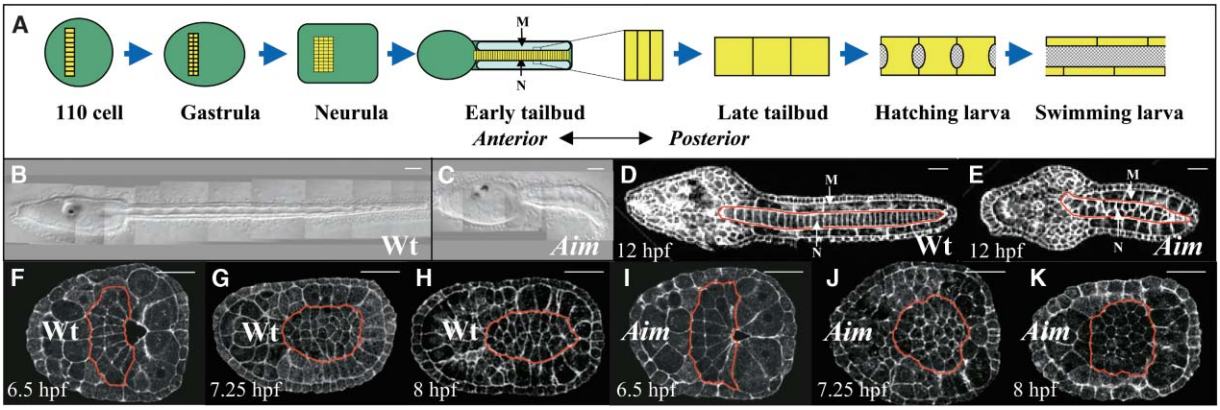

Figure 1. Notochord Morphogenesis Is Deficient in *aim* Embryos

(A) During gastrulation, C/E converts a four by ten sheet of developing notochord cells into a column of 40 stacked cells. Following C/E, notochord development continues as individual cells elongate in the A/P axis. M, muscle; N, notochord. (B and C) Normarski images of wild-type (B) and *aim* (C) tadpoles; lateral view, anterior to the left. (D–K) Confocal images of wild-type and *aim* embryos stained for filamentous actin (F-actin), which is enriched at the cortex of all notochord cells; dorsal view, anterior to the left. Scale bar, 50 μm.

Cs prickle (*Cs pk*), was found within this scaffold (Figure 2B). Because various PCP genes, including *pk*, have been implicated in vertebrate C/E [9–17], and in situ hybridization had shown that *pk* was expressed exclusively in developing notochord [18] (Figure 2D), *pk* was considered to be a strong candidate for the *aim* gene.

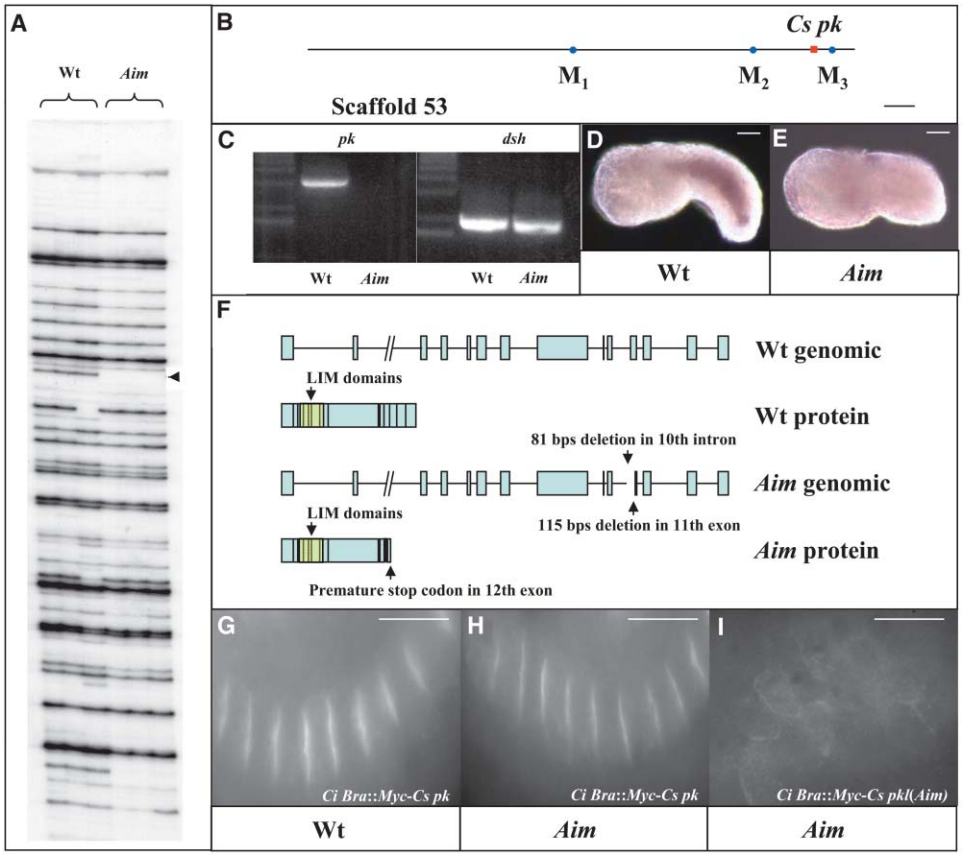

Figure 2. *Aim* Phenotype Is Caused by a Mutation in the *Cs pk* Gene

(A) AFLP-BSA analysis; arrow indicates linked band. (B) Linked markers and *Cs pk* in scaffold 53. Scale bar, 50,000 bp. (C–E) Expression of *Cs pk* is abolished in *aim* embryos at mid-tailbud stage as shown in RT-PCR assay (C), and in situ hybridization ([E]; compare with [D]); lateral view, anterior to the left. (F) Mutation in *Cs pk* genomic region and cDNA. (G–I) Immunohistochemical staining of Myc-tagged *Cs pk*. Expression of wild-type Myc-tagged *Cs pk* rescues *aim* phenotype ([H]; compare with [G]), while mutant version of *pk* fails to rescue (I); dorsal view, anterior to the left. Scale bar, 20 μm.

Both reverse transcription polymerase chain reaction (RT-PCR) and in situ hybridization failed to detect *Cs pk* expression in *aim/aim* embryos, although strong expression was observed in wild-type embryos (Figures 2C and 2E). Previous reports indicated that there were two *pk* genes in *C. intestinalis* [18]. However, more recently these have been found to be alternatively spliced forms of a single gene [19]. Similarly, the *C. savignyi* genome appears to contain a single *pk* gene.

Nucleotide sequencing of the *pk* gene from *aim/aim* embryos identified a 196 bp deletion that eliminated 81 bp of the 10th intron and 115 bp of the 11th exon. Using a more sensitive nested PCR protocol, we were able to amplify, at very low levels, the mutant *Cs pk* transcript and identify a premature stop codon in the 12th exon resulting from a frameshift due to the genomic deletion (Figure 2F and data not shown). The deletion found in the *pk* gene is predicted to result in a protein that is truncated following the three LIM domains and might not by itself create a null. However, the very low level of mutant *pk* transcript in *aim/aim* embryos (Figure 2C), perhaps a result of nonsense-mediated mRNA decay, would be expected to result in complete, or near-complete, loss of the *pk* gene product. A rescue construct was created to express wild-type *Cs pk* cDNA under the control of *Ciona intestinalis* (*Ci*) *brachyury* promoter in notochord cells [20] (Figure 2G). Expression of this construct rescued the *aim* phenotype (Figure 2H), while a similar construct expressing the mutant version of *pk* cDNA failed to rescue the phenotype (Figure 2I). Thus, we conclude that the *aim* phenotype is caused by a mutation in the *pk* gene.

Our observations of *aim/aim* embryos indicate an early defect in C/E, and *Cs pk* is expressed exclusively in the notochord, suggesting that *pk* controls some aspects of the C/E program. We therefore compared morphogenetic cell behaviors expressed during C/E in *aim* and wild-type notochord cells. Notochord precursor cells of the primary lineage were isolated from *aim/aim* and wild-type embryos at the 64- and 110-cell stages. Notochord isolates from *aim/aim* embryos at both stages showed the same cleavage pattern and schedule as the wild-type isolates, resulting in 32 notochord cells, as in wild-type (data not shown). During C/E, ascidian notochord cells become motile, extend actin-based lamellipodia, and align these protrusions preferentially parallel to mediolateral (M/L) axis [4]. The protrusion behavior of notochord cells isolated at the 64-cell stage was examined in detail. It was observed that notochord cells isolated from *aim/aim* embryos became motile and produced protrusions at the same frequency and of the same size as those produced by the cells from wild-type embryos (Figures 3A–3F). The ratio of lamellipodia extended by notochord cells along the M/L versus A/P axis at 7.25 hpf in situ was examined by confocal imaging, as described previously [4] (Figures 3G–3K). For wild-type embryos, a ratio of 2.2 was found, similar to what has been reported [4]. In contrast, the ratio was 1.2 for *aim/aim* embryos, indicating that the preference of notochord cells to send out protrusions along the M/L axis had been lost in the mutant. Thus, *pk* is not required for the normal expression of local protrusive activity but is required to resolve unbiased local protrusive activity into bipolar protrusion and C/E.

In *Drosophila*, PCP is established and maintained by the asymmetrical localization of PCP proteins [21–25]. In the wing disc, *frizzled* (*fz*) acts together with *stbm* and *flamingo* (*fmi*) to mediate apicolateral recruitment of PCP proteins, including *dsh* and *pk* [21, 23, 25, 26]. Later, *dsh* becomes localized at the distal end, while *pk* becomes localized at the proximal end of each cell. Several vertebrate PCP genes have been implicated in vertebrate C/E, including *dsh*, *pk*, and *stbm* [9–16, 27, 28]. However, asymmetrical localization of PCP factors in the midline tissues of developing chordate embryos has not been demonstrated. Furthermore, the interactions between chordate PCP proteins in regulating C/E are still largely unknown. The localization of *dsh* in ascidian notochord cells was examined at 8 hpf, a stage at which notochord cells are actively undergoing C/E, by expressing FLAG-tagged *Ci dsh* under the control of the *brachyury* promoter. We found that *dsh* was localized at the cell membrane, except where the cells were in contact with the presumptive muscle cells laterally (95%; n = 233) (Figures 3L and 3N). This result indicates that *dsh* is asymmetrically localized in the M/L axis of cells at the muscle/notochord boundary, suggesting intercellular signaling from neighboring cells, consistent with the observation that contact with neighboring tissues is required for notochord cell polarization [3]. No M/L polarization of *dsh* was observed in cells at the interior of the notochord field (Figures 3L and 3N), including in cases where the *dsh* reporter protein was expressed mosaically and thus expressing cells were surrounded by nonexpressing cells (data not shown). Surprisingly, *Ci dsh* and myc-tagged *Cs pk* colocalized at this stage (Figures 3L and 3M). In *aim/aim* embryos, *dsh* was found diffusely in the cytoplasm (Figure 3O) (87%; n = 245). Electroporation of a *Cs pk* cDNA construct rescued the mislocalization of *dsh* in *aim/aim* embryos (Figure 3P). Thus, *Cs pk* is required for membrane localization of *dsh* and M/L polarity of lateral notochord cells in the ascidian at the onset of C/E (Figure 3Q). In both *Xenopus* and ascidian, the muscle/notochord boundary is known to play an important role in facilitating C/E [3, 5]. Our data suggest that a signal at the notochord/muscle boundary may reduce both *pk* and *dsh* concentrations within notochord cells at that boundary, thereby establishing a M/L polarity that organizes bipolar protrusive activity across the width of the notochord.

The colocalization of *pk* and *dsh* in the ascidian notochord differs from the second and final phase of polarity establishment in the *Drosophila* wing disc, where *dsh* and *pk* are exclusive of each other, and from *dsh* expression in vertebrates, where *dsh* membrane localization is interrupted when exogenous *pk* is introduced [28]. On the other hand, our results resemble the initial phase of polarity establishment in the wing disc, where several PCP proteins, including *dsh* and *pk*, as well as *fz*, *stbm*, and *fmi*, form a protein complex that is localized at the membrane [23]. Other studies have also demonstrated the physical binding of *dsh* and *pk* [15, 25].

By early tailbud stage, after C/E is completed, *pk* was found to be localized to the boundary between adjacent notochord cells, but not at the lateral edges (Figure 2G). Examination of individual notochord cells from embryos

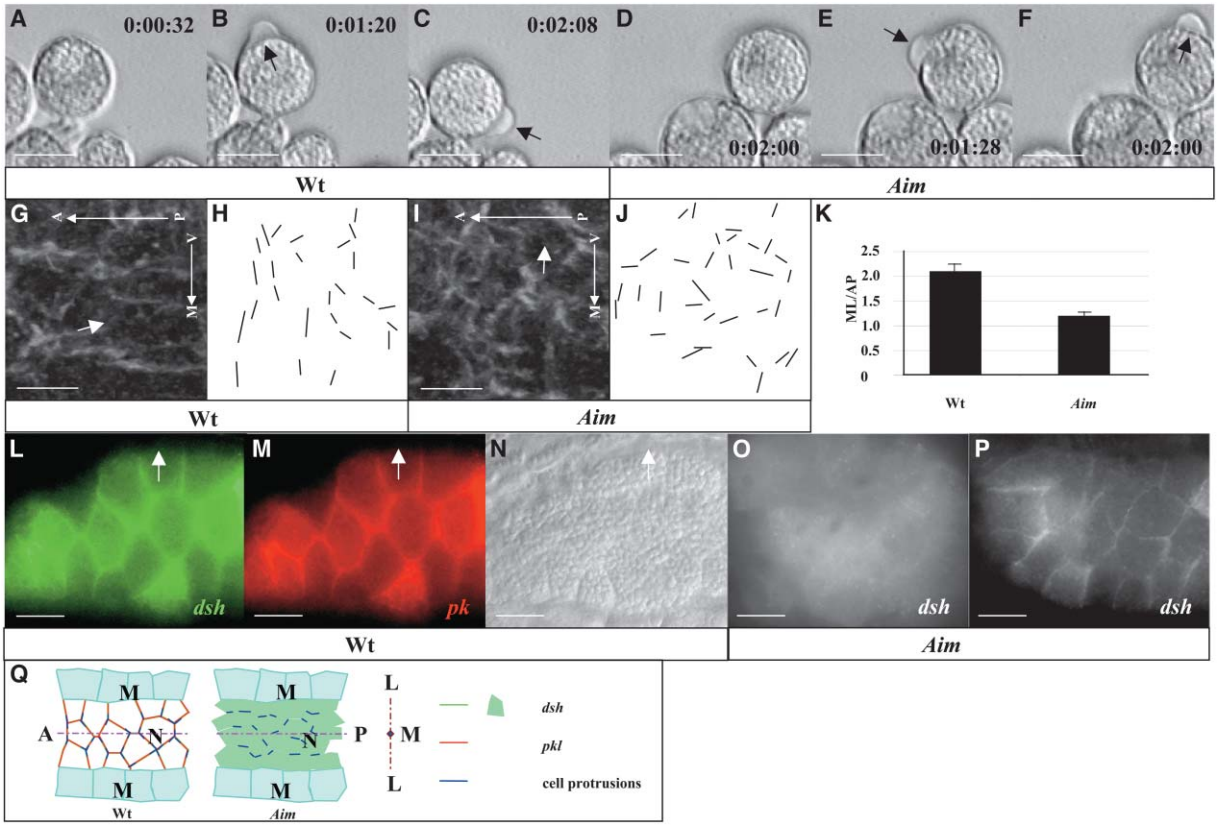

Figure 3. M/L Polarity of Notochord Cells Is Disrupted in *aim* Embryos

(A–F) Time-lapse images of isolated notochord cells show that cells from *aim/aim* embryos have the ability to extend lamellipodia (arrow). (G–J) Confocal images of actin-rich protrusions in notochord cells (dorsal view). Any protrusions that are within 45° angle from M/L axis are considered to have M/L directionality. (K) Summary of cell protrusions from 10 wild-type and 11 *aim* embryos reveals that the M/L directionality of notochord cells is lost in *aim* embryos. ML/AP, ratio of protrusions along M/L axis versus A/P axis. (L–N) Coelectroporation of FLAG-tagged *Ci dsh* (in green, [L]) and Myc-tagged *Cs pk* (in red, [M]) under the control of *Ci brachyury* promoter in wild-type notochord cells ([N]; Normarski view); arrowhead, boundary between notochord and muscle. Membrane localization of *dsh* is lost in *aim* notochord cells (O) and restored by coelectroporation of *Cs pk* (P). Dorsal view, anterior to the left. Scale bar, 10 μm. (Q) A model of ascidian notochord C/E regulated by *pk* and *dsh*. "N," notochord; "M," muscle.

mosaically expressing the FLAG-tagged *Ci pk* showed that *pk* was invariably localized at the anterior membrane (100%; n = 87) (Figure 4A). *Stbm*, which in *Drosophila* associates with *pk* during the establishment of planar cell polarity, was localized at both the anterior and posterior boundaries of cells (Figure 4B). In contrast, *dsh* at this same stage was localized predominantly along the notochord/muscle boundary (Figure 4C). After the early tailbud stage, the notochord cells begin to elongate along the A/P axis. By the late tailbud stage (16 hpf), *stbm*, like *dsh*, became predominantly localized at the anterior edge like *pk* (Figure 4E), although *pk* protein appeared to concentrate at the center of the cell (Figure 4D). The anterior localization of *pk* and *stbm* during the late tailbud stage notochord cells suggested a functional A/P polarization of the cells, although none has been described previously. One noticeable feature of the notochord cells at this stage was the asymmetric localization of the nuclei, which were positioned exclusively to the posterior end of each cell (Figures 4D′, D″, E′, and E″). The significance of the asymmetric position of the nuclei is unknown, but perhaps it is related to vacuole formation [1, 2]. Because the anterior localization of *pk* is the first sign of A/P polarity, we examined the requirement of *pk* for subsequent aspects of A/P polarity. To better visualize the nuclei, the *aim* line was crossed with a stable transgenic line expressing GFP under the control of the *Ci brachyury* promoter [29]. At late tailbud stage, GFP protein is accumulated at the cell membrane and the nucleus. In wild-type, all the nuclei are invariably positioned at the posterior end of each cell (Figure 4F), while nuclei in the *aim/aim* notochord cells were localized mostly, but not exclusively, at the anterior side (Figure 4G). One possibility is that the nuclei of notochord cells in *aim/aim* embryos require the earlier C/E event to bring the cells into a single file before the nuclei can be localized posteriorly. However, in approximately one-quarter of *aim/aim* embryos the posterior nine to ten notochord cells do form a single file, perhaps due to the constriction of the surrounding tissues. Nevertheless, the nuclei of these cells were mispositioned preferentially at the anterior side of notochord cells (82%; n = 113) (Figures 4I and I′; compare with 4H and H′). Taken together, these results demonstrate a new role for *pk* and the PCP pathway in polarizing midline cells along the A/P axis (Figures J–L).

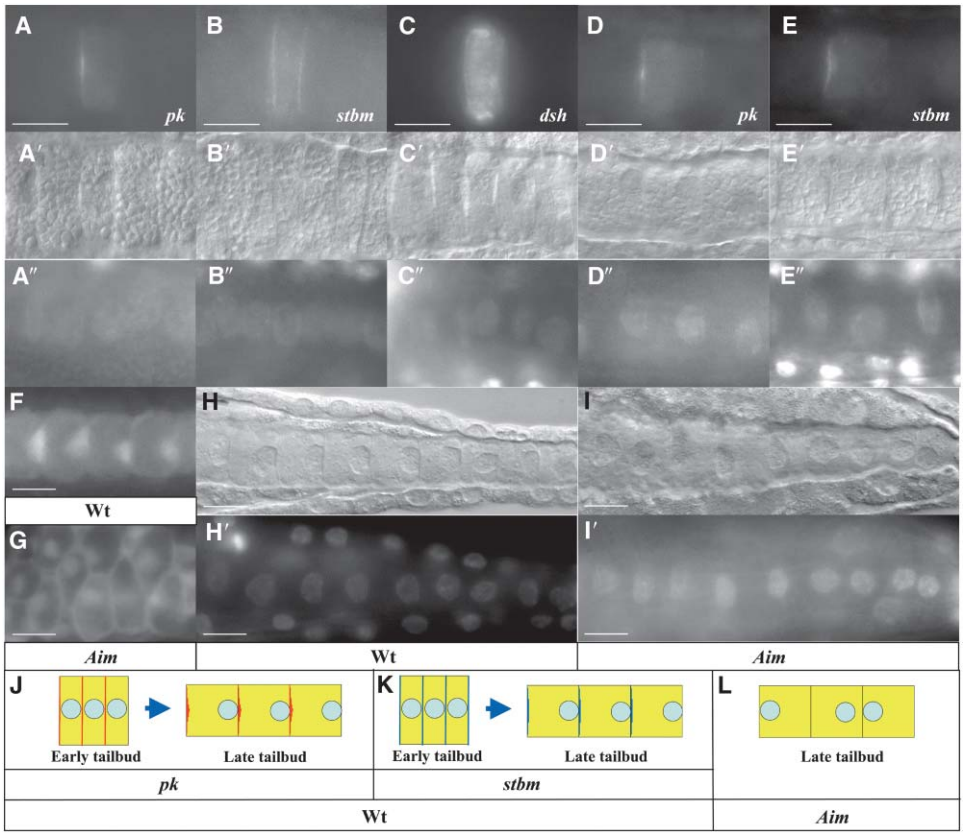

Figure 4. A/P Polarity of Individual Notochord Cells Is Disrupted in *aim* Mutant

(A–E) Localization of *pk*, *stbm*, and *dsh* at early tailbud (13 hpf; [A–C]) and late tailbud (16 hpf; [D and E]) stages. (A′–E′ and A″–E″) Normarski images and DAPI nuclear staining of the same cells in (A)–(E), respectively. (F and G) Notochord cells in stable transgenic embryos expressing GFP under the *Ci brachyury* promoter in wild-type (F) and *aim* background (G). (H, H′, I, and I′) Normarski images (H and I) and DAPI nuclear staining (H′ and I′) of posterior-most notochord cells in wild-type (H and H′) and *aim* (I and I′) embryos at late tailbud stage (16 hpf). Scale bar, 10 μm. (J–L) The reiterated A/P polarity of ascidian notochord cells requires PCP gene *pk*. All dorsal view, anterior to the left.

Conclusions

The defects observed in *aim/aim* embryos help to define the roles of *pk* and the PCP pathway in ascidian morphogenesis. Surprisingly, the loss of *pk* activity is not lethal to ascidians, and gastrulation, neurulation, and metamorphosis proceed without obvious problems. In the notochord, *pk* is essential for two aspects of M/L polarity: the M/L extension of lamellipodia, and asymmetrical membrane localization of *dsh* in lateral notochord cells that border the muscles. However, in the absence of *pk*, the motility of notochord cells, as indicated by the formation of lamellipodia, apparently was not altered. The fact that *dsh* did not appear to be polarized to non-border cells, despite these cells having polarized lamellipodia, suggests that the PCP pathway may only operate at the boundary and that some other mechanism relays polarized information to the interior cells. The present study also reveals an A/P polarity in notochord cells and that this polarity, like the M/L polarity, is dependent on *pk* activity. Finally, in vertebrates activation of the PCP pathway via frizzled is mediated by the signaling molecules wnt5a and wnt11 [30]. In *Ciona*, there appears to be a single wnt5 ortholog, and no wnt11 [31]. At the gastrula and neurula stages, when C/E is taking place, wnt5 is expressed in the muscle cells [32]. A second phase of wnt5 expression starts at the neurula stage and continues through tailbud stages and is concentrated at the posterior pole. Thus, the expression pattern of *Ciona* wnt5 is consistent with it playing a role in both M/L and A/P notochord cell polarity.

Experimental Procedures

Isolation of *aim*

Adult *C. savignyi* collected from the Santa Barbara yacht harbor were screened for spontaneous mutation by self-fertilization as described [8]. *Aim* was identified in a self-fertilized brood that was ~25% short-tailed. *C. savignyi* were maintained as previously described [8].

Histochemistry and Confocal Microscopy

C. savignyi embryos were fixed, stained with bodipy-phalloidin (Molecular Probes), and imaged by laser scanning confocal microscope (LSCM) as previously described [4]. To visualize actin-rich protrusions, LSCM Z series were collected at 0.2 μm intervals and imported into GraphicConverter X program (LEMKE Software) for further analysis [4]. Direction of cell protrusion was designated as M/L when it fell within a 45° angle from the body's M/L axis, seen from a dorsal view.

Molecular Cloning of *aim*

Three pools of 15 wild-type or mutant tadpoles from the self-fertilization of a single heterozygous *aim*/+ adult were collected to extract

genomic DNA for BSA experiments. AFLP was carried out using AFLP Analysis System II and AFLP Small Genome Primer Kit (Life Technologies) following the manufacturer's instruction. AFLP products were resolved on a 6% polyacrylamide gel; linked markers were isolated from the gel, amplified again using the original AFLP primer set, and cloned into pCR II Vector (Invitrogen) for sequencing, following standard protocols [33]. Sequences of linked markers were then blasted against the *C. savignyi* genome (http://www.broad.mit.edu/annotation/ciona/index.html) to obtain contigs that contain these markers. A translated BLAST search using the contig sequence against the GenBank protein sequence was performed to identify genes within the contigs. PCR primers covering consecutive regions of the entire *Cs pk* locus were used to survey both wild-type and *aim* genomic DNA by PCR and sequencing. Primers 5′-ATGAGTAG TCCTGCGATTTGTGGTA and 3′-TCTAGTTACCTGTATCGCATAT GCG identified a deletion in the last 1.8 kb region of *pk* in *aim*. We then performed 3′ rapid amplification of cDNA ends (RACE) on wild-type and *aim* cDNA using SMART RACE cDNA Amplification Kit (Clontech), with 5′-CCCCTTCCATTACCCCATCGCCCCCAACCA (pk17) and 5′-CCAAACACTTCCGCAACCGGGACCGAGGTT (pk19, nested primer for mutant *pk*), to obtain 3′ *pk* cDNA sequence and identified the resulting mutation in *aim* cDNA.

In Situ Hybridization and RT-PCR Analysis

Cs dsh was identified by a translated BLAST search of the *Ciona savignyi* genome (http://www.broad.mit.edu/annotation/ciona/index.html) using *Ci dsh* protein sequence. Specific primers, 5′-TCAAATT CAAACATGCCAGCGGTCGCAACTGAGCAGTTC (Cspk5), 3′-AAAA AGCGGCCGCTATCGCATATGCGAAGTAGAAGAAAAATT (Cspk3), 5′-ATGTCTGAAGAAGCGAAAATAGTT (Csdsh5), and 3′-TCACATGA CATCGACGAAGTAGTC (Csdsh3), were used to amplify fragments of *Cs pk* and *Cs dsh* from mid-tailbud stage wild-type and *aim* cDNA in RT-PCR. *Cs pk* fragment from wild-type was also cloned into pCR II Vector (Invitrogen) to generate probe for in situ hybridization, which was carried out as described [18].

Rescue

A Myc tag, flanked by BamHI and BglII, EcoRI sites, was inserted into pBS RN3 at the BglII and EcoRI sites to create pBS RN3 Myc. Full-length *pk* from wild-type and aim cDNA was amplified with primers 5′-GAGATCTTGAACATGCCAGCGGTCGCAACTGAGCAG TTC (pk28), 3′-TGCGGCCGCGAGCTCAGTTTTTCTATTTGGCTC (pk24), and 3′-TGCGGCCGCTCAGTTCATATCGACGTTTTTGCG (pk23, nested primer used for mutant *pk*) and cloned into pBS RN3 Myc at BglII and NotI sites to create Myc-*Cs pk* fusion constructs: pBS RN3 Myc-*Cs pk* and pBS RN3 Myc-*Cs pk*(*aim*). *Ci brachyury* promoter was amplified from *Ci-Bra*-TG [20] with 5′-AAGCTTCT GAACAAGCCATGTG (pCiBraTG5) and 3′-AAAGCTTTATAGGTTTG TAACTCGCACTGAG (pCiBraTG3) and inserted into pBS RN3 Myc-*Cs pk* and pBS RN3 Myc-*Cs pk*(*aim*) at HindIII site to create *Ci Bra*::Myc-*Cs pk* or *Ci Bra*::Myc-*Cs pk*(*aim*). Dechorionated eggs from in vitro cross-fertilization between two *aim* homozygous adults were electroporated with 100 μg of the above constructs and allowed to develop into late tailbud stage according to standard protocols [20]. Embryos were then fixed in cold methanol and cold ethanol, and notochord cells were visualize by immunohistochemical staining using anti-Myc antibody (Roche) followed by FITC anti-mouse antibody (Sigma) and fluorescent microscopy on Zeiss Isoskope 2 binocular microscope.

Time-Lapse Movie of Isolated Notochord Cells

Notochord precursors at 64-cell stage were isolated using a fine glass needle; cultured in Ca^{2+} and Mg^{2+} free seawater (0.9 M NaCl, 66 mM Na_2SO_4, 18 mM KCl, 5 mM $NaHCO_3$, 0.1 M Tris, and 5 mM disodium EDTA [pH 8.0]), on 0.1% gelatin- and 0.1% formaldehyde-coated slide; video-recorded every 8 s with a SPOT camera (Diagnostics Instrument, Inc.) attached to a LEICA binocular microscope, until the control whole embryos reached mid-tailbud stage. The individual images were encoded as time-lapse movies using Adobe Premiere (Adobe Systems Inc.).

Subcellular Localization of *dsh*, *pk*, and *stbm* in Notochord Cells

Full-length *Ci-dsh* was amplified from total *Ci* cDNA from tailbud stage with 5′-AGATCTGCCACCATGGATTACAAGGATGACGACGA TAAGTCGGATGAAACGAAAATAGTTTATTATCTT (dsh5′FLAG) and 3′-GCGGCCGCCTACATGACGTCAACAAAATAATCACACGG (dsh3′) and used to replace Myc-*Cs pk* in *Ci Bra*::Myc-*Cs pk*, at BglII and NotI sites, to create *Ci Bra*::FLAG-*Ci dsh*. Full-length *Ci stbm* was amplified from total *C. intestinalis* cDNA from tailbud stage embryos with 5′-AGATCTGCCACCATGGATTACAAGGATGACGACGATAAG GACACGGACAAATTACAAGACAATGATTCA (stbm5′FLAG) and 3′-GCGGCCGCTCACACCGACGTCTCGCTCTGCATGTGCAT (stbm3′) and used to construct *Ci Bra*::FLAG-*Ci stbm* as for *dsh*. For coexpression of *Cs pk* and *Ci dsh*, 50 μg of each construct was electroporated simultaneously. *Dsh* localization was visualized by immunohistochemistry using anti-FLAG antibody (Sigma) followed by TRITC anti-rabbit antibody (Sigma). To generate isolated notochord cells expressing the construct, we used 20–50 μg of DNA in electroporation.

Acknowledgments

We wish to thank Dr. Gaku Kumano for helpful discussion and Dr. George von Dassow for technical assistance. This work was supported by a grant from the National Institutes of Health (HD38701) to W.C.S.

Received: September 27, 2004
Revised: November 15, 2004
Accepted: November 16, 2004
Published: January 11, 2005

References

1. Satoh, N. (1994). Developmental Biology of Ascidians (Cambridge: Cambridge University Press).
2. Miyamoto, D.M., and Crowther, R.J. (1985). Formation of the notochord in living ascidian embryos. J. Embryol. Exp. Morphol. *86*, 1–17.
3. Munro, E.M., and Odell, G. (2002). Morphogenetic pattern formation during ascidian notochord formation is regulative and highly robust. Development *129*, 1–12.
4. Munro, E.M., and Odell, G.M. (2002). Polarized basolateral cell motility underlies invagination and convergent extension of the ascidian notochord. Development *129*, 13–24.
5. Keller, R., Davidson, L., Edlund, A., Elul, T., Ezin, M., Shook, D., and Skoglund, P. (2000). Mechanisms of convergence and extension by cell intercalation. Philos. Trans. R. Soc. Lond. B Biol. Sci. *355*, 897–922.
6. Nishida, H. (1987). Cell lineage analysis in ascidian embryos by intracellular injection of a tracer enzyme. III. Up to the tissue restricted stage. Dev. Biol. *121*, 526–541.
7. Di Gregorio, A., and Levine, M. (1999). Regulation of Ci-tropomyosin-like, a Brachyury target gene in the ascidian, Ciona intestinalis. Development *126*, 5599–5609.
8. Hendrickson, C., Christiaen, L., Deschet, K., Jiang, D., Joly, J.-S., Legendre, L., Nakatani, Y., Tresser, J., and Smith, W.C. (2004). Culture of adult ascidians and ascidian genetics. In Development of Sea Urchins, Ascidians, and Other Invertebrate Deuterostomes: Experimental Approaches, C.A. Ettensohn, G.M. Wessel, and G.A. Wray, eds. (San Diego, CA: Academic Press), pp. 143–169.
9. Wallingford, J.B., Rowning, B.A., Vogeli, K.M., Rothbacher, U., Fraser, S.E., and Harland, R.M. (2000). Dishevelled controls cell polarity during Xenopus gastrulation. Nature *405*, 81–85.
10. Wallingford, J.B., Fraser, S.E., and Harland, R.M. (2002). Convergent extension: the molecular control of polarized cell movement during embryonic development. Dev. Cell *2*, 695–706.
11. Park, M., and Moon, R.T. (2002). The planar cell-polarity gene stbm regulates cell behaviour and cell fate in vertebrate embryos. Nat. Cell Biol. *4*, 20–25.
12. Wallingford, J.B., and Harland, R.M. (2002). Neural tube closure

requires Dishevelled-dependent convergent extension of the midline. Development *129*, 5815–5825.
13. Darken, R.S., Scola, A.M., Rakeman, A.S., Das, G., Mlodzik, M., and Wilson, P.A. (2002). The planar polarity gene strabismus regulates convergent extension movements in Xenopus. EMBO J. *21*, 976–985.
14. Goto, T., and Keller, R. (2002). The planar cell polarity gene strabismus regulates convergence and extension and neural fold closure in Xenopus. Dev. Biol. *247*, 165–181.
15. Takeuchi, M., Nakabayashi, J., Sakaguchi, T., Yamamoto, T.S., Takahashi, H., Takeda, H., and Ueno, N. (2003). The prickle-related gene in vertebrates is essential for gastrulation cell movements. Curr. Biol. *13*, 674–679.
16. Veeman, M.T., Slusarski, D.C., Kaykas, A., Louie, S.H., and Moon, R.T. (2003). Zebrafish prickle, a modulator of noncanonical Wnt/Fz signaling, regulates gastrulation movements. Curr. Biol. *13*, 680–685.
17. Jenny, A., Darken, R.S., Wilson, P.A., and Mlodzik, M. (2003). Prickle and Strabismus form a functional complex to generate a correct axis during planar cell polarity signaling. EMBO J. *22*, 4409–4420.
18. Hotta, K., Takahashi, H., Asakura, T., Saitoh, B., Takatori, N., Satou, Y., and Satoh, N. (2000). Characterization of Brachyury-downstream notochord genes in the Ciona intestinalis embryo. Dev. Biol. *224*, 69–80.
19. Sasakura, Y., Yamada, L., Takatori, N., Satou, Y., and Satoh, N. (2003). A genomewide survey of developmentally relevant genes in Ciona intestinalis. VII. Molecules involved in the regulation of cell polarity and actin dynamics. Dev. Genes Evol. *213*, 273–283.
20. Corbo, J.C., Levine, M., and Zeller, R.W. (1997). Characterization of a notochord-specific enhancer from the Brachyury promoter region of the ascidian, Ciona intestinalis. Development *124*, 589–602.
21. Strutt, D.I. (2001). Asymmetric localization of frizzled and the establishment of cell polarity in the *Drosophila* wing. Mol. Cell *7*, 367–375.
22. Axelrod, J.D. (2001). Unipolar membrane association of Dishevelled mediates Frizzled planar cell polarity signaling. Genes Dev. *15*, 1182–1187.
23. Bastock, R., Strutt, H., and Strutt, D. (2003). Strabismus is asymmetrically localised and binds to Prickle and Dishevelled during Drosophila planar polarity patterning. Development *130*, 3007–3014.
24. Tree, D.R., Ma, D., and Axelrod, J.D. (2002). A three-tiered mechanism for regulation of planar cell polarity. Semin. Cell Dev. Biol. *13*, 217–224.
25. Tree, D.R., Shulman, J.M., Rousset, R., Scott, M.P., Gubb, D., and Axelrod, J.D. (2002). Prickle mediates feedback amplification to generate asymmetric planar cell polarity signaling. Cell *109*, 371–381.
26. Axelrod, J.D., Miller, J.R., Shulman, J.M., Moon, R.T., and Perrimon, N. (1998). Differential recruitment of Dishevelled provides signaling specificity in the planar cell polarity and Wingless signaling pathways. Genes Dev. *12*, 2610–2622.
27. Jessen, J.R., Topczewski, J., Bingham, S., Sepich, D.S., Marlow, F., Chandrasekhar, A., and Solnica-Krezel, L. (2002). Zebrafish trilobite identifies new roles for Strabismus in gastrulation and neuronal movements. Nat. Cell Biol. *4*, 610–615.
28. Carreira-Barbosa, F., Concha, M.L., Takeuchi, M., Ueno, N., Wilson, S.W., and Tada, M. (2003). Prickle 1 regulates cell movements during gastrulation and neuronal migration in zebrafish. Development *130*, 4037–4046.
29. Deschet, K., Nakatani, Y., and Smith, W.C. (2003). Generation of Ci-Brachyury-GFP stable transgenic lines in the ascidian Ciona savignyi. Genesis *35*, 248–259.
30. Wallingford, J.B. (2004). Closing in on vertebrate planar polarity. Nat. Cell Biol. *6*, 687–689.
31. Hino, K., Satou, Y., Yagi, K., and Satoh, N. (2003). A genomewide survey of developmentally relevant genes in Ciona intestinalis. VI. Genes for Wnt, TGFβ, Hedgehog and JAK/STAT signaling pathways. Dev. Genes Evol. *213*, 264–272.
32. Imai, K.S., Hino, K., Yagi, K., Satoh, N., and Satou, Y. (2004). Gene expression profiles of transcription factors and signaling molecules in the ascidian embryo: towards a comprehensive understanding of gene networks. Development *131*, 4047–4058.
33. Ransom, D.G., and Zon, L.I. (1999). Mapping zebrafish mutations by AFLP. In The Zebrafish: Genetics and Genomics, Volume 60, H.W. Detrich III, M. Westerfield, and L.I. Zon, eds. (San Diego, CA: Academic Press), pp. 195–212.